
Authors

P. Justin Jesuraj, Chuanqian Shi, Dong Hyun Kim, Hassan Hafeez, Jong Chan Lee, Won Ho Lee, Dae Keun Choi, Zhanan Zou, Jianliang Xiao, Jeongho Min, Myungkwon Song, Chang Su Kim, and Seung Yoon Ryu

Direction-dependent stretchability of AgNW electrodes on microprism-mediated elastomeric substrates

Cite as: AIP Advances **8**, 065227 (2018); <https://doi.org/10.1063/1.5026742>

Submitted: 23 February 2018 . Accepted: 21 June 2018 . Published Online: 29 June 2018

P. Justin Jesuraj, Chuanqian Shi , Dong Hyun Kim, Hassan Hafeez, Jong Chan Lee , Won Ho Lee, Dae Keun Choi, Zhanan Zou, Jianliang Xiao, Jeongho Min , Myungkwan Song , Chang Su Kim, and Seung Yoon Ryu 



View Online



Export Citation



CrossMark

ARTICLES YOU MAY BE INTERESTED IN

[Programmable localized wrinkling of thin films on shape memory polymers with application in nonuniform optical gratings](#)

Applied Physics Letters **112**, 251603 (2018); <https://doi.org/10.1063/1.5037120>

[Simultaneous formation of multiscale hierarchical surface morphologies through sequential wrinkling and folding](#)

Applied Physics Letters **112**, 081602 (2018); <https://doi.org/10.1063/1.5020177>

[Aerosol jet printed silver nanowire transparent electrode for flexible electronic application](#)

Journal of Applied Physics **123**, 174905 (2018); <https://doi.org/10.1063/1.5028263>

AVS Quantum Science

Co-published with AIP Publishing



Coming Soon!

Direction-dependent stretchability of AgNW electrodes on microprism-mediated elastomeric substrates

P. Justin Jesuraj,^{1,a} Chuanqian Shi,^{2,3,a} Dong Hyun Kim,^{1,a} Hassan Hafeez,¹ Jong Chan Lee,¹ Won Ho Lee,¹ Dae Keun Choi,¹ Zhanan Zou,² Jianliang Xiao,^{2,b} Jeongho Min,⁴ Myungkwan Song,⁴ Chang Su Kim,^{4,b} and Seung Yoon Ryu^{1,b}

¹*Division of Display and Semiconductor Physics, Display Convergence, College of Science and Technology, Korea University Sejong Campus, 2511 Sejong-ro, Sejong City 30019, Republic of Korea*

²*Department of Mechanical Engineering, University of Colorado, 427 UCB, Boulder, CO 80309-0427, USA*

³*School of Aerospace Engineering and Applied Mechanics, Tongji University, Shanghai 200092, China*

⁴*Advanced Functional Thin Films Department, Korea Institute of Materials Science (KIMS) Changwon 51508, Republic of Korea*

(Received 23 February 2018; accepted 21 June 2018; published online 29 June 2018)

Silver nanowires (AgNWs) have become an efficient electrode candidate for stretchable electronics. We report the effects of directional stretching in microprism-mediated AgNW stretchable electrodes on polyurethane (PU) substrates. The wavy substrate is fabricated using a customized microprism on polyethylene terephthalate. AgNWs on stretchable PU substrates show stable normalized resistance up to 35% strain under parallel uniaxial stretching. This performance is much better than AgNWs on bare PU substrate or on wavy PU under perpendicular stretching, which can only sustain 10%-15% strain before significant increase in normalized resistance. Finite element simulations were conducted to reveal the strain distribution and variation in the AgNW electrodes on both bare and wavy PU substrates when stretched along parallel and perpendicular directions. Comparing to AgNW electrodes on bare PU and on wavy PU under perpendicular stretching, the wavy PU surface relief features can effectively alleviate the strain in the AgNW network when stretched along parallel direction, leading to better performance. © 2018 Author(s). All article content, except where otherwise noted, is licensed under a Creative Commons Attribution (CC BY) license (<http://creativecommons.org/licenses/by/4.0/>). <https://doi.org/10.1063/1.5026742>

I. INTRODUCTION

Stretchable electrodes with high conductivity under more strain are essential for various applications including stretchable displays,^{1,2} wearable electronics,³ smart textiles,⁴ and flexible solar cells.⁵ Notably, for display applications, electrodes should exhibit a stable conductivity of at least 10%–30% strain;⁶ Several exotic candidates have been applied as electrode materials to achieve this task, such as metal thin films, carbon nanotubes, graphene, and metal nanowires (NWs).^{7–14} Recently, metal NW-based electrodes deliver better performance than the other materials owing to its flexible nature at a macroscopic scale.¹⁴ Silver nanowires (AgNWs) and AgNWs polymer composites offer enhanced performance in stretchable electrode applications; however, their activity entirely depends on the tedious fabrication process.^{15–17}

In general, electrode materials are deposited on the buckling structures or vertical waviness created on polymer substrates, which sustain the cracks under strain. To create buckling structures on

^aThese authors contributed equally to this paper.

^bCorresponding author list: Prof. Dr. SeungYoon Ryu, Tel: +82-44-860-1376, justie74@korea.ac.kr; Dr. Chang Su Kim, cskim1025@kims.re.kr; and Prof. Dr. Jianliang Xiao, jianliang.xiao@colorado.edu



polymer, it is cured on pre-stretched elastomeric substrates. Formation of an elastomeric substrate is achieved using metal forms,⁷ hollow fibers,¹⁸ and microfluidic channels.¹⁹ To realize better performance and fewer defects, microprism-mediated pre-stretched elastomeric substrates are used for preparing stretchable polymer substrates. Due to the Poisson effect between the polymer and the electrode material, wrinkles or cracks⁷⁻⁹ appear on the electrode during stretching. In addition, if the direction of stretching is changed, the effects of Poisson ratio variation between the material and the substrate will be more. Further, variation in the properties of the elastomeric substrate or the coating direction can also trigger alterations in stretchable electrode performance.^{20,21} For example, Ko *et al.*²⁰ found that AgNW alignment on a polydimethylsiloxane (PDMS) substrate induces many changes in the NW junction formation, which consequently affects the electrode sheet resistance and overall performance. Kim *et al.*¹² demonstrated the need of a proper slope and height of the microprism buckling structure on the PDMS substrate for achieving very high stretching ability. Thus, careful selection of elastomeric substrate parameters is essential for better electrode performance.

In this context, we investigated the effects of stretching direction on the performance of AgNW-coated polyurethane (PU) stretchable electrodes. The possible Poisson effect variation with respect to parallel and perpendicular stretching direction was discussed. To support the experimental results, a simulation based on finite element analysis (FEA) was conducted to realize the strain effect variation in different parts of the substrate under variable loads and stretching direction.

II. EXPERIMENTAL

A wavy PU substrate was prepared by coating PU solution on a microprism-mediated polyethylene terephthalate (PET) substrate; the detailed experimental process is schematically illustrated in Fig. 1. The microprisms on the PET substrate were obtained by acrylic resin forming of one-dimensional prism structures whose pitch was a few tens of micrometers²² (in our case it was 44 μm). After the PU dispersion, the solution was cured at room temperature for 24 h to improve adhesion. Then, the peeled PU contained wavy structures, similar to that in the microprism-mediated PET substrate. This wavy PU substrate did not contain any cracks or defects, as shown in Fig. 2, thus confirming the controlled processing of a buckled PU substrate. The commercially purchased (C3NANO) AgNW solution (consisting of NWs with 20 nm diameter and 20 μm length) in ethanol with a concentration of 0.3 wt% was spin coated on to the buckled PU substrate at a speed of 800 RPM for 1 min. Further, the sample was annealed at 100°C for 1 min to remove the solvent moieties. The uniformity of the AgNWs on the wavy PU substrate was studied by field emission-scanning electron microscopy (FE-SEM) and the transmission characteristics were verified using ultraviolet-visible spectroscopy. The stretchable characteristics of the AgNW electrode was measured by calculating the normalized resistance ($\Delta R/R_0$, where ΔR is change in resistance and R_0 is initial resistance) with

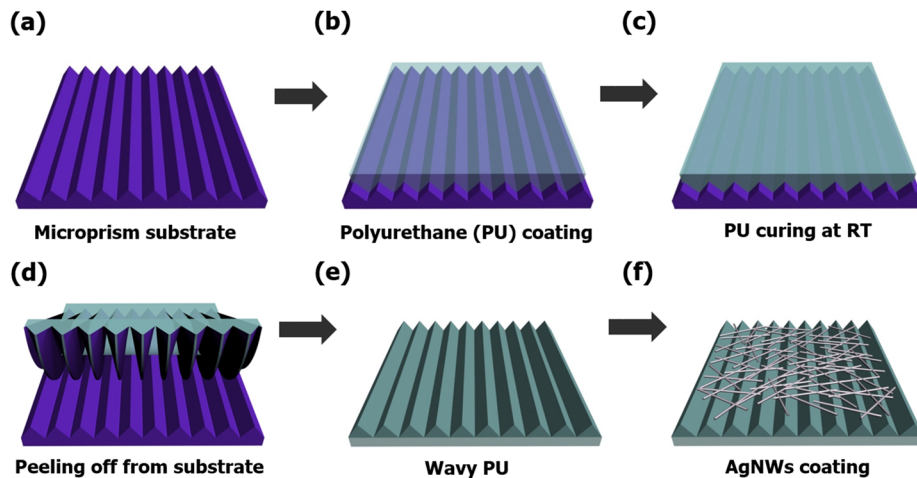


FIG. 1. Processing of PU stretchable electrodes with AgNWs from microprism templates.

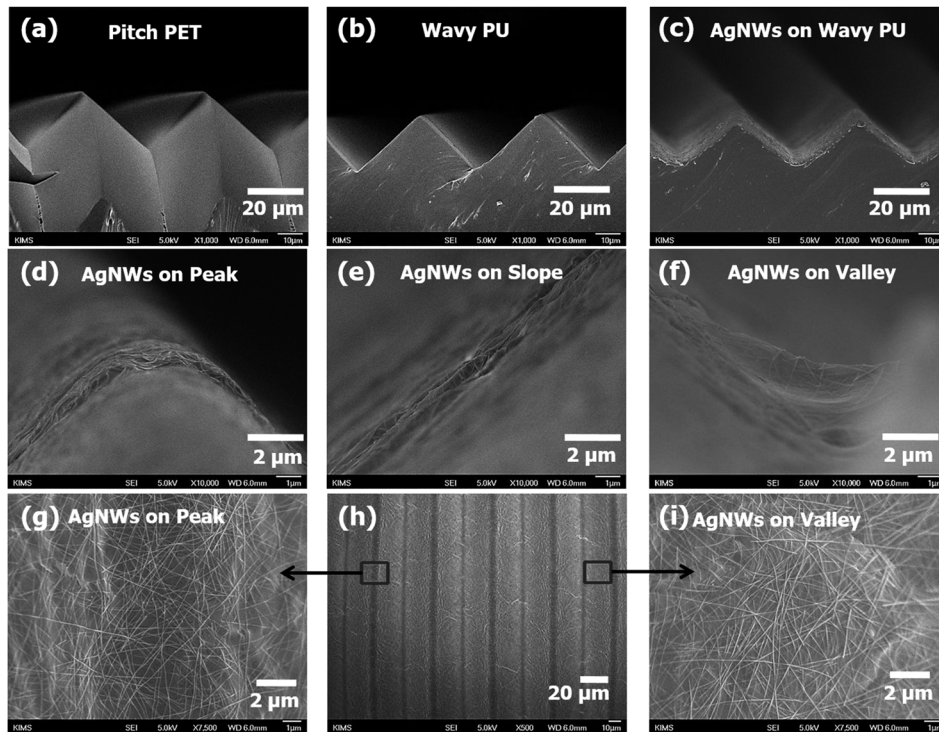


FIG. 2. FE-SEM cross-sectional images of (a) microprism pitch and wavy PU surface (b) before and (c) after AgNW coating. Deposition of AgNWs at (d) peak, (e) slope, and (f) valley points of wavy PU. (g), (h), and (i) Bird's-eye views of AgNWs at the peak and valley points of PU.

respect to various applied strain values. A customized setup to induce strain was attached with a multimeter to monitor the corresponding change in resistance under different strain conditions. To understand the experimentally observed electrode performances, finite element simulations using commercial software ABAQUS were conducted to compare the strain distribution in the AgNWs on the bare and wavy PU substrate under the parallel and perpendicular stretching directions.

III. RESULTS AND DISCUSSION

Fig. 2(a)–2(c) display the cross-sectional views of PET, wavy PU, and AgNW-coated PU substrates, respectively. Further, in magnified view (Figs. 2(d)–2(f), the images clearly showed that the coating of AgNWs was uniform at the peak, slope, and valley positions, respectively. The abovementioned positions with bird's view are shown in Figs. 2(g)–(i). The density of AgNWs was slightly higher at the valley points than at the peak areas. The NWs intersected to form junctions, which helped to realize conductivity in the AgNW electrode. The transmission characteristics of the AgNW-coated wavy PU substrate and bare PU substrate is illustrated in Fig. 3. After spin coating the NWs on the PU substrate, transmission decreased from 90% to 70% at 550 nm. The naked view of the substrate is shown in the inset of Fig. 3.

The stretchable characteristics of the AgNW-coated bare PU substrate (without wavy shape) were measured by calculating the sheet resistance of the substrate with respect to various values of applied strain, as shown in Fig. 4. Significantly, the performance of the AgNWs with respect to parallel (denoted as “X”) and perpendicular (denoted as “Y”) stretching directions of the wavy PU shape (pitch 44 μm) was also investigated. During the stretching, the Poisson effect variation between the AgNWs and the PU substrate resulted in the formation of cracks and wrinkles. For example, the AgNW-coated bare PU substrate exhibited stable normalized resistance (change in sheet resistance) of up to 10%–12% strain only. If the strain was increased beyond 12%, the normalized resistance values varied exponentially. Poisson's ratio of the AgNWs (~ 0.2 or less) is lower than that of PU

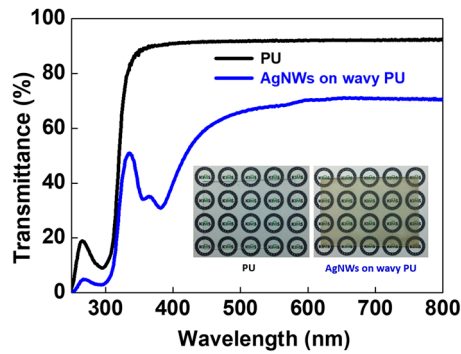


FIG. 3. Transmittance characteristics of PU substrate with and without AgNWs. The slight reduction occurred on transmission of PU is attributed to the higher density of AgNWs. However, the electrode offers more than 70% transmission in the visible spectrum. The inset of figure is the naked view of the substrate.

(~ 0.5); hence, the former induces a higher friction between the surfaces, resulting in the formation of cracks that eventually break the NW junction.^{23,24} Hence, the conductivity of the AgNWs decreased after a certain value of the applied strain.

However, in the case of the wavy PU substrate, the conductivity of the AgNWs was retained up to 35% strain in the parallel stretching. The micropriam-mediated pre-strained wavy PU substrate clearly decreased the strain applied to the AgNWs by distributing the applied strain systematically. During the strain, the maximum force is acting on the valley region whereas, relatively lower force experienced at peak. Hence, breaking of the NW junction at the peak areas were comparatively less and the conductivity of the AgNW electrode was maintained until 35% strain. The results were successfully reproduced more than 5 times. When the direction of stretching was changed to the Y direction, the strain variation in the NW substrate was completely different. Because, during Y axis based stretching the strain on the substrate was almost uniform. That is, the orientation of the buckling structures on the wavy electrode and the applied strain in the Y direction were along the same axis. Hence, the strain applied along the Y axis could not be compensated by the buckling structures and the amount of strain was expected to be equal at the peak as well as valley points of the electrode. As a result, a larger decrease in conductivity was observed for the AgNW electrode. However, Fig. 4 demonstrates that even under perpendicular stretching, the AgNW electrode exhibited sustainability and low change in resistance up to 15% strain, which was better than that of bare PU-based electrodes.

To corroborate the effects of stretching on the AgNW electrode, the morphology of the AgNW-coated PU substrates was monitored after 40% strain, as shown in Fig. 5. The AgNW-coated bare

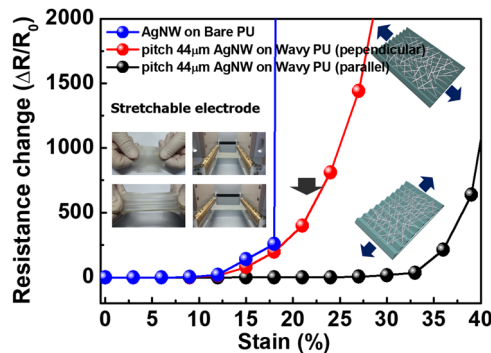


FIG. 4. Performance of stretchable electrodes. Variation in sheet resistance with respect to strain applied along different directions to AgNWs deposited on wavy PU surfaces. The performance of AgNWs coated on bare PU substrate is also compared. The insets of figure are stretching photos and the schematic illustration of AgNWs deposited on wavy PU electrodes.

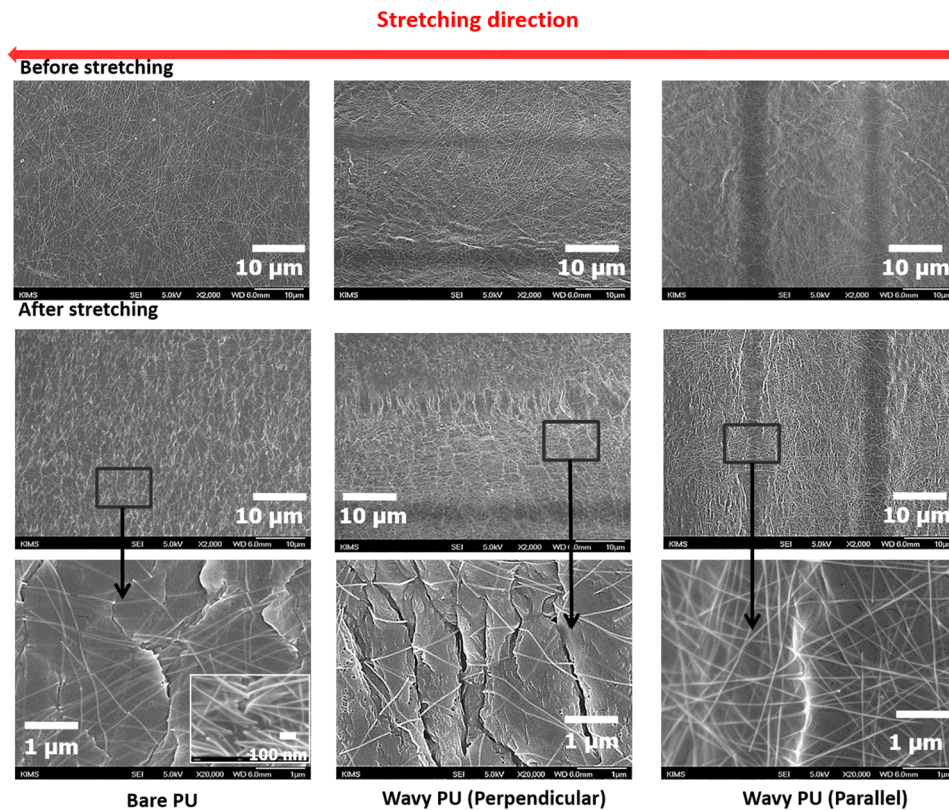


FIG. 5. Comparison of FE-SEM images of AgNW-coated PU substrate before and after strain analysis. The effects of X and Y directional stretching together with bare PU substrate performance are also compared.

PU substrate underwent certain cracks on its surface, which expectedly broke the NW junctions and resulted in reduced conductivity. Electrodes subjected to perpendicular stretching also exhibited visual cracks and wrinkles on their surface, eventually leading to breaks in the AgNW network and hence reduced conductivity. However, the electrodes with the wavy PU surface subjected to parallel stretching revealed high stability up to 35% strain condition. There were no visible cracks observed in the FE-SEM micrograph, thus proving the enhanced performance of the AgNW electrode under parallel stretching. During this parallel stretching, the Poisson effect was expected to be suppressed by the applied pressure through periodic wave patterns and hence high stretching ability was achieved. Thus, the AgNW-coated wavy PU substrate could be employed as an electrode for stretchable lighting devices. Usually, the valley points in wavy electrodes are subjected to more strain during parallel stretching, whereas the peak points are most affected during perpendicular stretching, as shown in Fig. 5. However, under perpendicular stretching, because of the Poisson ratio difference between the AgNWs and the PU substrate, the entire electrode starts to shrink, even under small strain, resulting in breakage of the NW junction, especially at the peak points. Hence, the resistance change under perpendicular stretching is higher than under parallel stretching.

To get more insight into the electrode performance, the PU substrate was modelled as an isotropic material using 3D strain elements (C3D8R), as shown in Fig. 6(a). Its Young's modulus and Poisson's ratio were $E_m = 5$ MPa and $\nu_m = 0.47$, respectively. The AgNW film was modelled as a bilayer short fiber composite using shell elements (S4R) due to their (NWs) short lengths and large aspect ratios. The film was bonded at the top of the PU substrate, as shown in Fig. 6(a). Its Young's modulus and Poisson's ratio were $E_f = 140$ GPa and $\nu_f = 0.23$, respectively. The two composite laminates were perpendicular to each other, each of thickness 50 nm, as schematically shown in Fig. 6(b). For each short fiber composite layer, the material's properties could be calculated using the Halpin-Tsai

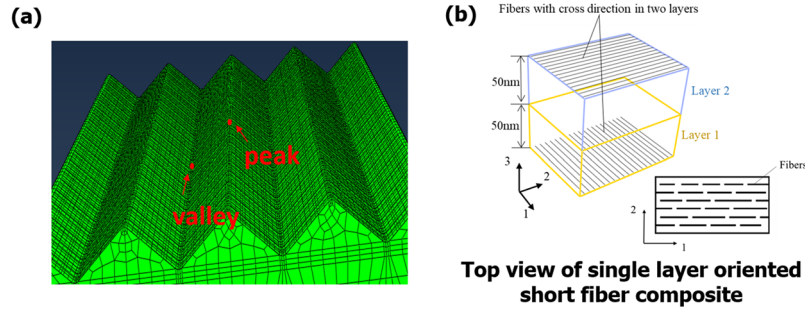


FIG. 6. (a) Illustration of PU substrate using 3D stress elements; (b) the modeling of bilayer composite laminate for the AgNW film.

equations:²⁵

$$E_{11} = \frac{E_f(1 + 2\alpha V_f) + E_m(1 - 2\alpha V_f)}{E_f V_m + E_m(1 + V_f)} E_m, \quad (1)$$

$$E_{22} = \frac{E_f(1 + 2V_f) + E_m(1 - 2V_f)}{E_f V_m + E_m(1 + V_f)} E_m, \quad (2)$$

$$G_{12} = \frac{G_f(1 + V_f) + G_m V_m}{G_f V_m + G_m(1 + V_f)} G_m, \quad (3)$$

$$G_{23} = \frac{G_f \left(1 + \frac{1 + \nu_m}{3 - \nu_m - 4\nu_m^2} V_f \right) + G_m \left(1 - \frac{1 + \nu_m}{3 - \nu_m - 4\nu_m^2} V_f \right)}{G_f V_m + G_m(1 + V_f)} G_m, \quad (4)$$

$$\nu_{12} = \nu_f V_f + \nu_m V_m, \quad (5)$$

where subscripts 1, 2, and 3 represent the longitudinal, transverse, and out-of-plane directions, respectively; α is the length-diameter ratio of the AgNWs; V_f and V_m are the volume ratios of the AgNW film and PU matrix, respectively; and G_f and G_m are the shear moduli of the AgNW film and PU matrix, respectively. The average diameter and length of the NWs were estimated to be 20 nm and 20 μ m, respectively, giving the length-diameter ratio $\alpha = 1000$. In a cross-sectional area of 100 nm by 50 nm, there were estimated to be three NWs, which gives the volume ratio of NWs to be $V_f = 0.19$. Based on these parameters, the material's properties were calculated to be $E_{11} = 2161.58$ MPa, $E_{22} = 7.16$ MPa, $G_{12} = 2.43$ MPa, G_{23} (G_{13}) = 2.54 MPa, and $\nu_{12} = 0.42$.

Fig. 7(a)–(d) exhibit the FEA simulation results of strain distribution in the AgNW electrodes, based on the Halpin-Tsai equations. The strains on the electrodes experienced at the valley and peak positions of the prism wavy substrate with 40% and 10% strain load is depicted in Fig. 7. When subject to perpendicular stretching, the strain in the electrode is much higher than parallel stretching. It coincides with the experimental results. Wavy substrate under 40% strain load in perpendicular direction demonstrated the highest strain generation. To better compare strain distributions in different cases, we used the same scale bars for the contours in Fig. 7(a) and (c)–(f). However, due to the very high strain with 40% load along perpendicular direction, Fig. 7(b) used a different scale bar for clarity. In comparison to perpendicular stretching, prism substrate under parallel stretching offers much lower strain owing to the presence of periodic prism surface relief patterns.

We have also conducted FEA simulations to compare our stretchable prism wavy patterns with a sinusoidal wavy²⁶ pattern of the same electrode thickness and pattern wavelength and amplitude, as shown in Figs. 7(e) and (f). When stretched by 10% along the parallel direction, the strain distribution in the sinusoidal wavy pattern is similar to that in our prism wavy structure. However, when stretched by 40% along the parallel direction, the maximum strain in the electrode on the sinusoidal wavy pattern (13.4%) is higher than that in the electrode on the prism pattern (10.5%). This suggests that our prism pattern can provide better stretching performance than sinusoidal wavy pattern. At this

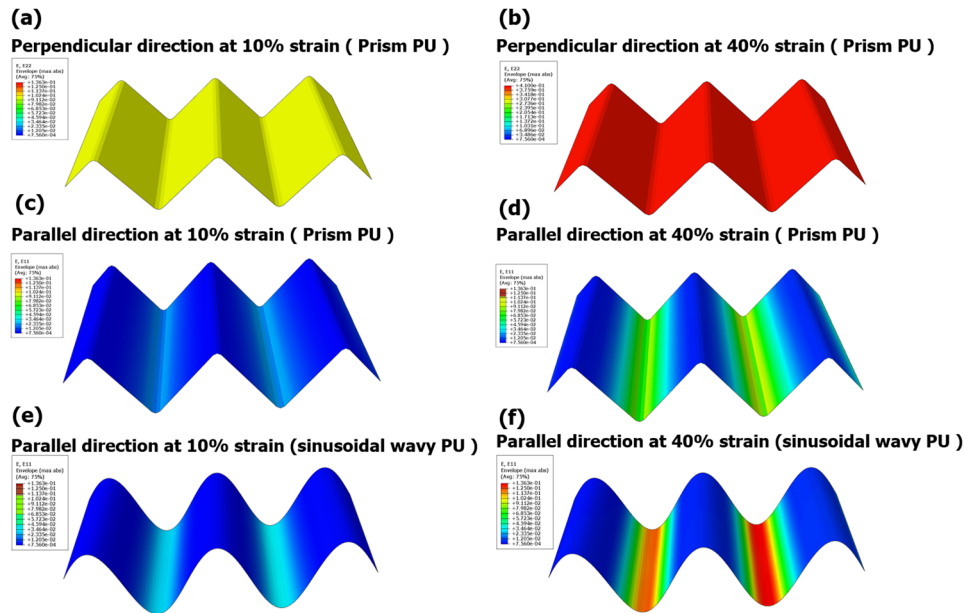


FIG. 7. The simulated strain distribution mapping observed at the peak and valley points of the PU/AgNW electrode with 10% and 40% strain loads, under (a)-(b) perpendicular direction stretching, (c)-(d) parallel stretching. (e) and (f) show the parallel stretching based strain distribution in uniform sinusoidal wavy PU under 10% and 40% loads.

strain load, prism wavy substrate exhibits strong and confined strain at the valley line perpendicular to the stretching direction. This confined strain generation together with lower values compared with sinusoidal wavy structures are beneficial to avoiding the nanowire junction breakage and give better conductivity. Hence, the structure proposed here with prism wavy patterns could be helpful to fabricate stretchable electrodes with lower strain generation in parallel stretching. It was reported in an earlier study that AgNW electrodes could be stretched by 60% or more.²⁶ This was due to that the buckling induced sinusoidal wavy pattern can provide stretchability up to the strain used to induce buckling and nanowire junction sliding allows relative motion among AgNWs without breaking conductive paths. Our method, however, provides an alternative to the buckling strategy that doesn't require generation of buckling, but directly coat fabricated prism substrates with conductive AgNW films. This method offers more freedom to control the surface relief structure, including wavelength and amplitude, for design and optimization purposes.^{27,28}

The estimated strain values at the peak and valley points with respect to plus strain along the X and Y directions for prism wavy patterns are presented in Fig. 8(a). Strain values were estimated

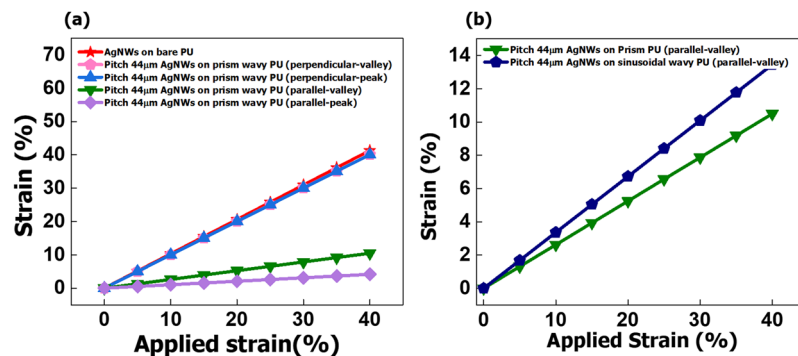


FIG. 8. (a) The estimated strain in AgNW electrode calculated at the peak and valley points versus applied strain under stretching along two directions and (b) comparison of valley points strain under parallel stretching in prism and uniform sinusoidal wavy substrates based AgNWs.

in the middle part of the substrate to prevent abrupt results arising from estimation at the boundaries of the substrate. In the perpendicular direction, the strain was observed at the peak and valley points and strain on the bare PU substrate was found to be similar. In addition, compared to parallel stretching, perpendicular stretching induced very poor stability of electrode, which confirms our experimental observations. Thus, the AgNW junctions formed on the PU substrates subjected to severe load on perpendicular stretching showed relatively weak stability. In the case of parallel stretching, the simulation predicted that the strain observed at the valley points was higher than that at the peak points. As explained in the above discussions, we derived that the difference between Young's modulus and Poisson's ratio of the PU substrate and AgNWs caused a strain variation, which provoke the breakage of the NW junctions and hence reduced the conductivity. This effect is more in perpendicular stretching as compare to parallel strain. Therefore, the relative resistance change was better under parallel stretching. Furthermore, Fig. 8(b) displays the comparisons of strain at valley points of sinusoidal wavy and prism wavy substrates. It confirms the conclusion mentioned above that prism substrates provide lower strain than sinusoidal wavy patterns. Thus, the theoretical simulations clearly confirmed the AgNW electrode performance under parallel and perpendicular stretching.

IV. CONCLUSION

In summary, AgNW-based stretchable electrodes were fabricated on microprism-mediated pre-stretched PU substrates. The uniformity of AgNW deposition on the wavy PU surface was examined by FE-SEM. Further, the transparency of the electrode was confirmed after the deposition of AgNWs. The variation in normalized resistance with respect to various stretching directions was investigated. The bare PU surface coated with AgNWs was stable until 10% strain. However, the wavy PU AgNW electrode offered stability up to 35% strain under parallel stretching. When the stretching direction was changed to perpendicular, the electrode stability was maintained only up to 15% strain. The stability and NW junction breakage were also investigated using the FE-SEM images. Further, detailed theoretical simulations using FEA were applied to quantify the strain variation observed at the peak and valley points of the electrode. The prism wavy pattern was compared with widely used sinusoidal wavy substrates. It was shown that when stretched along the perpendicular direction the prism and sinusoidal wavy patterns offer similar stretching performance, but when stretched along the parallel direction, the prism pattern provides better stretching performance than the sinusoidal wavy substrates.

ACKNOWLEDGMENTS

This research was supported by the Basic Science Research Program through the National Research Foundation of Korea (NRF) funded by the Ministry of Education (NRF-2014R1A6A1030732, 2016R1A6A1A03012877, and 2017R1A2B4005583). This research was also supported by the Pioneer Research Center Program through the National Research Foundation of Korea funded by MSIP (NRF-2013M3C1A3065525).

- ¹ T. Sekitani, H. Nakajima, H. Maeda, T. Fukushima, T. Aida, K. Hata, and T. Someya, *Nature Materials* **8**(6), 494–499 (2009).
- ² J. A. Rogers, T. Someya, and Y. Huang, *Science* **327**(5973), 1603–1607 (2010).
- ³ B. W. An, E.-J. Gwak, K. Kim, Y.-C. Kim, J. Jang, J.-Y. Kim, and J.-U. Park, *Nano Letters* **16**(1), 471–478 (2015).
- ⁴ F. Axisa, P. M. Schmitt, C. Gehin, G. Delhomme, E. McAdams, and A. Dittmar, *IEEE Transactions on Information Technology in Biomedicine* **9**(3), 325–336 (2005).
- ⁵ F. C. Krebs, S. A. Gevorgyan, and J. Alstrup, *Journal of Materials Chemistry* **19**(30), 5442–5451 (2009).
- ⁶ W. Hu, X. Niu, L. Li, S. Yun, Z. Yu, and Q. Pei, *Nanotechnology* **23**(34), 344002 (2012).
- ⁷ J. Jeong, S. Kim, J. Cho, and Y. Hong, *IEEE Electron Device Letters* **30**(12), 1284–1286 (2009).
- ⁸ Y. U. Ko, S.-r. Cho, K. S. Choi, Y. Park, S. T. Kim, N. H. Kim, S. Y. Kim, and S. T. Chang, *Journal of Materials Chemistry* **22**(8), 3606–3613 (2012).
- ⁹ N. Saran, K. Parikh, D.-S. Suh, E. Muñoz, H. Kolla, and S. K. Manohar, *Journal of the American Chemical Society* **126**(14), 4462–4463 (2004).
- ¹⁰ H.-Z. Geng, K. K. Kim, K. P. So, Y. S. Lee, Y. Chang, and Y. H. Lee, *Journal of the American Chemical Society* **129**(25), 7758–7759 (2007).
- ¹¹ B. Dan, G. C. Irvin, and M. Pasquali, *ACS Nano* **3**(4), 835–843 (2009).
- ¹² K.-H. Kim, D.-W. Jeong, N.-S. Jang, S.-H. Ha, and J.-M. Kim, *RSC Advances* **6**(62), 56896–56902 (2016).

- ¹³ N. Chou, Y. Kim, and S. Kim, [ACS Applied Materials & Interfaces](#) **8**(9), 6269–6276 (2016).
- ¹⁴ Y. Yang, S. Ding, T. Araki, J. Jiu, T. Sugahara, J. Wang, J. Vanfleteren, T. Sekitani, and K. Suganuma, [Nano Res.](#) **9** (2016).
- ¹⁵ M. Amjadi and I. Park, presented at the Nanotechnology (IEEE-NANO), 2014 IEEE 14th International Conference on, 2014 (unpublished).
- ¹⁶ M. K. Shin, J. Oh, M. Lima, M. E. Kozlov, S. J. Kim, and R. H. Baughman, [Advanced Materials](#) **22**(24), 2663–2667 (2010).
- ¹⁷ C. W. Park, S. W. Jung, S. C. Lim, J.-Y. Oh, B. S. Na, S. S. Lee, H. Y. Chu, and J. B. Koo, [Microelectronic Engineering](#) **113**, 55–60 (2014).
- ¹⁸ S. Zhu, J. H. So, R. Mays, S. Desai, W. R. Barnes, B. Pourdeyhimi, and M. D. Dickey, [Advanced Functional Materials](#) **23**(18), 2308–2314 (2013).
- ¹⁹ K. P. Mineart, Y. Lin, S. C. Desai, A. S. Krishnan, R. J. Spontak, and M. D. Dickey, [Soft Matter](#) **9**(32), 7695–7700 (2013).
- ²⁰ Y. Ko, S. K. Song, N. H. Kim, and S. T. Chang, [Langmuir](#) **32**(1), 366–373 (2015).
- ²¹ G. S. Jeong, D.-H. Baek, H. C. Jung, J. H. Song, J. H. Moon, S. W. Hong, I. Y. Kim, and S.-H. Lee, [Nature Communications](#) **3**, ncomms1980 (2012).
- ²² J. H. Lee, (Google Patents, 2010).
- ²³ R. Widdle, A. Bajaj, and P. Davies, [International Journal of Engineering Science](#) **46**(1), 31–49 (2008).
- ²⁴ E. K. McCarthy, A. T. Bellew, J. E. Sader, and J. J. Boland, [Nature Communications](#) **5** (2014).
- ²⁵ C. L. Tucker III and E. Liang, [Composites Science and Technology](#) **59**(5), 655–671 (1999).
- ²⁶ F. Xu and Y. Zhu, [Advanced Materials](#) **24**(37), 5117–5122 (2012).
- ²⁷ J. Xiao, A. Carlson, Z. Liu, Y. Huang, H. Jiang, and J. Rogers, [Applied Physics Letters](#) **93**(1), 013109 (2008).
- ²⁸ Y. Wang, Z. Li, and J. Xiao, [Journal of Electronic Packaging](#) **138**(2), 020801 (2016).